Method for producing correct fingerprints

S. Madhusudana Rao

Department of Instrumentation, Indian Institute of Science, Bangalore 560 012, India

madhu@isu.iisc.ernet.in

Received 19 July 2007; revised 4 November 2007; accepted 11 November 2007;
posted 12 November 2007 (Doc. ID 85117); published 20 December 2007

The conventional method of producing fingerprints by total internal reflection using a right-angle prism does not give true size images. In this case an anamorphic real image is formed by the Scheimpflug condition with keystone distortion. A method of combining a single prism with the right-angle prism for anamorphic stretching to get the correct fingerprint image is described. The method of constructing such a type of an optical system is discussed in detail. The method is useful to directly obtain the correct fingerprints using a CCD camera.

OCIS codes: 350.4600, 220.4830.

1. Introduction

The use of fingerprints [1,2] for identification purposes has been known for the past several years. High-contrast fingerprints are made by placing the finger on the diagonal face of a right-angle (45°–90°–45°) prism (RP) as shown in Fig. 1. In this total internal reflection (TIR) method the prism–finger interspace is illuminated by the light beam with an elliptical cross section. The major axis of the ellipse is along the length of the diagonal face of the prism. The reflected beam from the prism–finger interspace emerges with a circular cross section from the side face of the RP. This light beam carries the lengthwise information of the fingerprint in a compressed form. The compression factor in this case is $1/\sqrt{2}$. The real images of such fingerprints are formed by anamorphic stretching under Scheimpflug conditions [3–5]. According to [4], the Scheimpflug imaging (i.e., imaging with tilted object and image planes with respect to the optic axis of the lens) produces keystone distortion. To correct this defect several researchers have developed systems using holographic techniques and fiber optics components [6–11]. Some of them [6,8–10] have called this defect a trapezoidal distortion. They have mentioned that this type of distortion can be corrected by additional optics or by using the appropriate software to correct the fingerprint images. Stephany and Haas [12], have suggested a method to correct the keystone aberration in image storage systems. Duran-Ramirez and Malacara-Doblado [13] have suggested methods to correct keystone distortion in overhead projectors. In this paper a totally different method is suggested to produce correct fingerprints.

The use of prisms for anamorphic magnification was first suggested by Brewster [14] in 1831 and further developments in this subject were made by several researchers [15–21]. The use of a wedge prism as an anamorphic beam expander along with the RP (Fig. 1), for restoring the actual size of the fingerprint free from distortion, is discussed and the experimental results are presented in this paper.

2. Conventional and Proposed Methods for Producing Fingerprints

The schematic of a conventional fingerprint recording apparatus is shown in Fig. 2. Usually the optical system is arranged in a box with two rectangular openings, one containing the diagonal face of the RP for placing fingers, and the other opening containing a ground glass screen for observation, exactly in the place of photographic film of Fig. 2. The optical system of Fig. 2 works at a very high magnification. Only a portion of the fingerprint can be imaged on a large photographic plate with this apparatus. For the purpose of imaging the entire fingerprint on a 35 mm film at lower magnification, the optical system of Fig. 2 is modified as shown in Fig. 3. In Figs. 2 and 3, the

0003-6935/08/010025-05$15.00/0

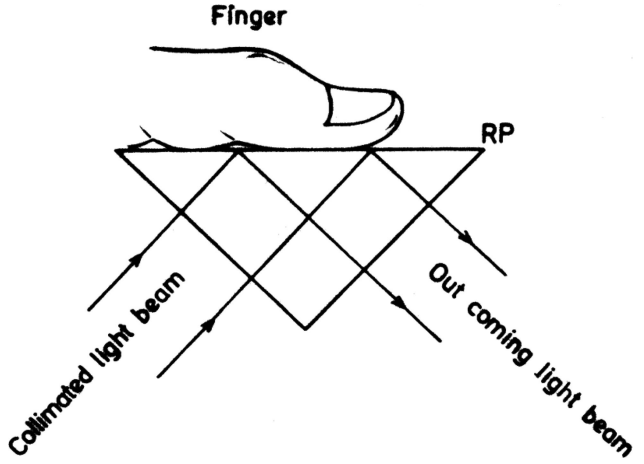

Fig. 1. Typical RP used for producing high-contrast fingerprints.

plane mirror is used for forming the image on a ground glass screen for convenient viewing from the top. If the plane mirror is removed, the image can be formed on a ground glass screen (or film) placed inclined to the axis of the camera lens. The Scheimpflug method is an anamorphic imaging system. More details on this subject are discussed in [4].

The RP of Fig. 1 is the basic optical component for producing high-contrast fingerprints by the TIR method. In this case the light beam has an elliptical cross section at the finger–prism interface (on the diagonal face of the RP). The same light beam emerges from the side face of the RP with a circular cross section. The lengthwise information of the fingerprint is compressed by a factor of $1/\sqrt{2}$. The real images are formed by Scheimpflug conditions using the experimental arrangements shown in Figs. 2 and 3. In this method the cross section of the light beam is anamorphically stretched on the image planes of Figs. 2 and 3. Keystone distortion occurs in Scheimpflug imaging [4]. To understand the image formation in Figs. 2 and 3, we have redrawn the basic equivalent optical system as shown in Fig. 4. In this diagram the tilted object plane O and image plane I represent the diagonal face of the RP and the photographic film plane of Fig. 3. Let us consider the object plane containing a grid pattern as shown in Fig. 5. The grid pattern is placed in the object plane O in such a way that the horizontal

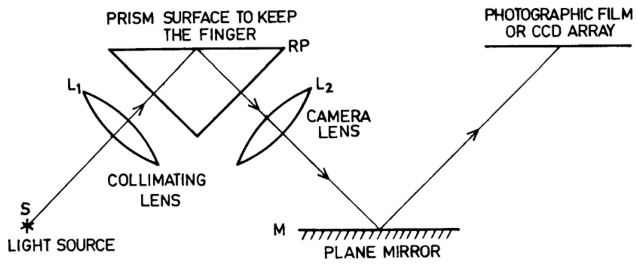

Fig. 2. Schematic of the optical system used in conventional fingerprint apparatus that works at very high magnification.

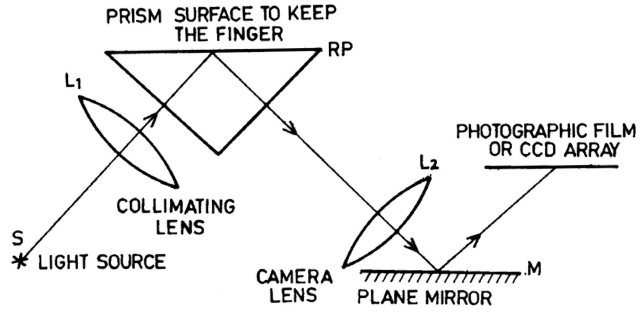

Fig. 3. Schematic of the modified optical system that works at lower magnification.

lines are parallel to the X axis of Fig. 4. The periodic spacing of the grid pattern is equal. The components of vertical periods in a plane perpendicular to the optic axis (Z axis) are all equally compressed by a factor of $1/\sqrt{2}$. This plane corresponds to the light exit face of the RP in Fig. 3. If the object at O is imaged on the tilted image plane I, we get the image as shown in Fig. 6. This image is produced by placing the grid pattern of Fig. 5, on the diagonal face of RP of the optical system shown in Fig. 3. This image has keystone distortion. The detailed procedure to place the grid pattern on the diagonal face of the RP is discussed in the foregoing sections. In Fig. 4 even though the object plane O is tilted, the object can also be imaged in a plane perpendicular to the optic axis indicated by the dashed line I′. This case is implemented by imaging the same grid object in a plane perpendicular to the optic axis of Fig. 3. The resulting image is shown in Fig. 7. We see from Fig. 7, that the vertical periods of the grid lines are uniformly compressed by a factor of $1/\sqrt{2}$. We found that it is possible to correct the image by adding an additional optical element for anamorphic stretching with a magnification factor of $\sqrt{2}$, and imaging in a plane perpendicular to the optic axis.

The method to restore the elliptical shape of the light beam internally reflected from the diagonal face of the RP, and forming the correct images of the fingerprints, is shown in Fig. 8. In this experimental arrangement the correcting prism (CP) is a single-element anamorphic beam expander. The method of designing such a system is discussed in Subsection 2.A.

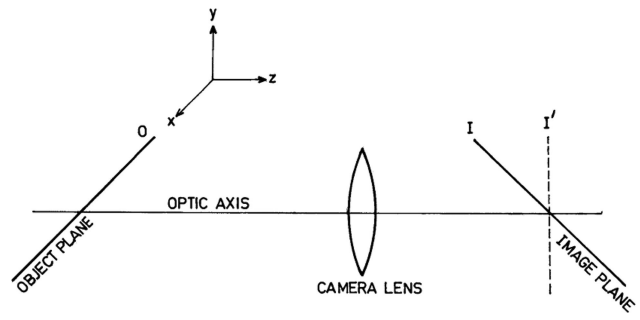

Fig. 4. Simplified equivalent diagram of Fig. 3.

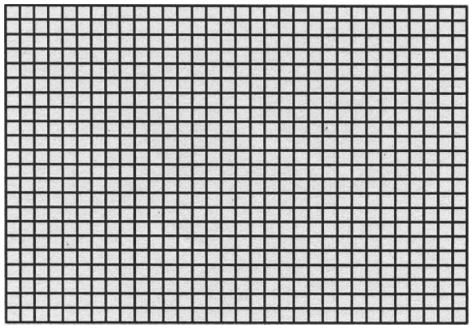

Fig. 5. Diagram of the periodic grid pattern used in experiments.

A. Single Prism Anamorphic Beam Expander

The proposed method to correct the fingerprint is shown in Fig. 8. In this case the emerging light beam from the RP enters the CP at an angle D with respect to the horizontal axial line (parallel to the base of the CP). The angle of incidence on the first surface of the CP is equal to $A + D$, where A is the apex angle of the prism. The light ray is refracted at an angle equal to A inside the CP and emerges out from the second surface along its normal. If we imagine that the light ray is traveling from right to left, the angle D can be called an angle of deviation. The relation between the angles D and A can be given as

$$D = \arcsin(n \sin A) - A. \tag{1}$$

The mathematical expression for anamorphic magnification M produced by the CP can be given according to [19] as

$$M = \frac{\cos A}{(1 - n^2 \sin^2 A)^{1/2}}, \tag{2}$$

where n is the refractive index of CP. This equation leads to the following relation for prism angle A:

$$A = \arcsin\left(\frac{M^2 - 1}{M^2 n^2 - 1}\right)^{1/2}. \tag{3}$$

In the present case $M = \sqrt{2}$. Substituting the values of M and n in Eq. (3) prism angle A can be calculated. The angle D can be calculated from Eq. (1).

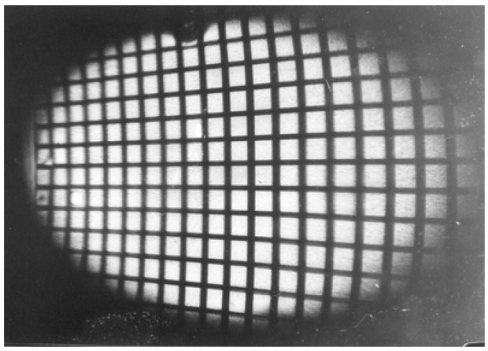

Fig. 6. Photographic image of the grid pattern of Fig. 5, produced from the optical system shown in Fig. 3.

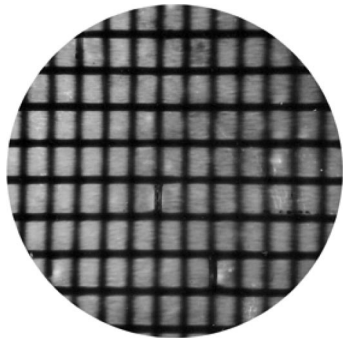

Fig. 7. Photographic image of the same grid pattern (Fig. 5) obtained by making the image plane (photographic film) perpendicular to the optic axis in Fig. 3.

B. Experimental Details

We have made a borosilicate crown glass prism CP with $n_d = 1.5097$ and angle $A = 32° 50'$. This CP is placed in the experimental setup as shown in Fig. 8. The CP is aligned with respect to the RP, using accurately machined jigs. A grid pattern (Fig. 5) with horizontal and vertical lines having 2 mm separation (period), is generated by a printed circuit board (PCB) design software. The grid was printed on a lithographic film (0.11 mm thick) using a photoplotting machine. The grid pattern is placed on the diagonal face of the RP (meant for placing the finger) after placing few drops of isopropyl alcohol both on the cleaned prism surface and also on the printed side of the grid pattern. The pattern is moved sidewise till the air bubbles and excess alcohol come out and it is pressed tightly against the prism surface. The procedure is just the same as wringing slip-gauges to one another or to a glass surface. In this case the printed ink on grid pattern was not dissolved by alcohol. The pattern remained in tact for nearly 5 h.

The experimental photographs of the grid images, produced using the two optical systems (Figs. 3 and 8) are shown as Figs. 6 and 9. After removing the grid

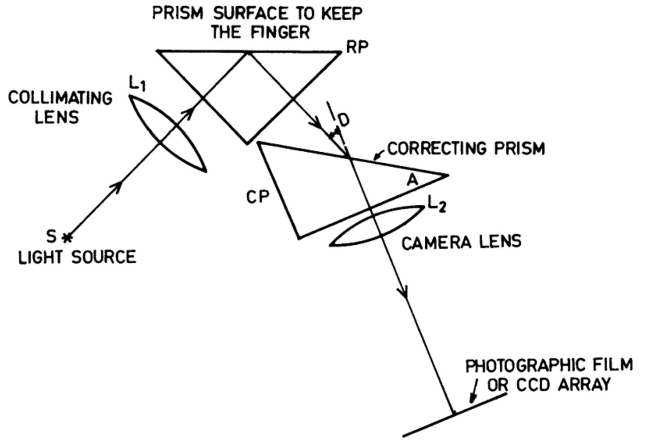

Fig. 8. Schematic of the proposed alternate system consisting of a combination of a RP and a single-prism anamorphic beam expander CP for restoring the fingerprint to its true size without distortion.

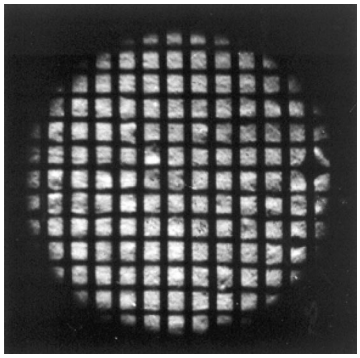

Fig. 9. Photographic image of the grid pattern of Fig. 5 obtained from the proposed optical system shown in Fig. 8.

pattern, the diagonal face of the RP is cleaned. The experiments are conducted for producing the fingerprints with the same two optical arrangements. Figures 10 and 11 illustrate the experimental results. Figures 6 and 10 are produced by the conventional method of imaging (as shown in Fig. 3). Figures 9 and 11 are produced from the proposed experimental setup as shown in Fig. 8.

C. Discussion of the Results

From Fig. 6 we understand that there is no constant uniform magnification in the image plane if we use the setup shown in Fig. 3. The experimental systems of Figs. 3 and 8 are just adjusted to photograph the images on a 35 mm film. The experimental setup shown in Fig. 8 is adjusted for minimization of the image by a factor of 0.67. This is with reference to the size of the object on the prism surface. It has nothing to do with the magnification factor $\sqrt{2}$ used for the design of the CP (Fig. 8). Figures 9 and 11 are the experimental results for this case. The periodic separations of the grid pattern on the photographic negative of Fig. 6 are measured along the central horizontal and vertical lines. The results of the measurements are given in Table 1. If we look at the experimental results of Table 1 corresponding to Fig. 6, there is no uniform spacing between the grid line images. Also in Fig. 6 the horizontal lines on either side of the centerline are found to be inclined at 6.1°, 5.5°, 3.9°, 2.6°, and 1.38° angles. This indicates the presence of keystone distortion. The average periodic separations of the horizontal and vertical grid lines on the negative of Fig. 9 are also measured. These results are given in Table 2. The second and fourth columns of Table 2 (corresponding to Fig. 9) are the results obtained by dividing first and second column results by the minimization factor 0.67. If we compare these results with the 2 mm line spacing, of the grid pattern (Fig. 5), we find that the keystone distortion is almost eliminated.

Fig. 10. Photographic image of the fingerprint produced from the conventional optical system shown in Fig. 3.

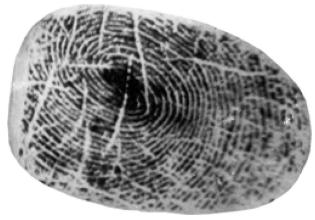

Fig. 11. Photographic image of the same fingerprint (Fig. 10) produced from the proposed optical system shown in Fig. 8.

From the above discussions and from Figs. 6 and 9, we find that the conventional method of Scheimpflug imaging produces a considerable amount of keystone distortion that is not present in Fig. 9, produced by the modified optical system shown in Fig. 8. If we look at the fingerprint images of Figs. 10 and 11, we observe that the fingerprint of Fig. 10 has nonuniform magnification due to keystone distortion. The fingerprint given in Fig. 11 is the image produced from the optical system shown in Fig. 8. This is for the same finger shown in Fig. 10, restored to true size without distortion. The image of the same fingerprint impression on a plane paper is given in Fig. 12.

In the experimental arrangements shown in Figs. 3 and 8, collimated light beam enters the camera lens. In the former case (Fig. 3) the light beam leaving the RP contains the object information in anamorphically compressed form. In the latter case (Fig. 8) the light bundle leaving the CP contains the object information restored to its original dimensions. If we count the number of vertical lines in Fig. 9, and look at the

Table 1. Measured Separations of the Grid Lines on the Photographic Negative of Fig. 6 along the Central Horizontal and Vertical Lines

Horizontal (mm)	Vertical (mm)
0.99	1.65
1.12	1.62
1.13	1.60
1.15	1.60
1.17	1.59
1.20	1.58
1.24	1.60
1.28	1.62
1.32	1.67
1.40	1.70
1.48	1.73
1.56	1.75
1.60	
1.70	
1.90	
1.92	
1.88	
1.90	

Table 2. Measured Average Separations of the Grid Lines on the Photographic Negative of Fig. 9 for Horizontal and Vertical Lines

Horizontal		Vertical	
(mm)	After Division by 0.67 (mm)	(mm)	After Division by 0.67 (mm)
1.33	1.98	1.37	2.04
1.37	2.04	1.38	2.06
1.34	2.00	1.35	2.01
1.37	2.04	1.38	2.06
1.34	2.00	1.36	2.03
1.34	2.00	1.37	2.04
1.36	2.03	1.39	2.07
1.33	1.98	1.37	2.04
1.34	2.00	1.39	2.07
1.33	1.98	1.36	2.03
1.39	2.07	1.39	2.07

2 mm line spacing of the grid (Fig. 5), we can understand that the diameters of the front, rear components of the camera lens (25 and 22 mm) restrict the length of the fingerprint to be imaged with the arrangement shown in Fig. 8. If we observe Figs. 6 and 9 the above statement is true. If we want to produce a fingerprint covering a greater length of the finger, we may have to use a camera lens with a larger aperture. If the focal length of the camera lens increases the experimental system occupies more space.

For our experimental setups shown in Figs. 3 and 8, we have used a lens with focal length 75 mm and 30 mm diameter for collimating the light beam. The light beam entry and exit faces of the RP (Figs. 1–3 and 8) have approximate dimensions of 46.5 mm $\times$ 47 mm. The diagonal face of the RP has approximate dimensions of 64 mm $\times$ 47 mm. The light bundle entry face of the CP (Fig. 8) has approximate dimensions of 60 mm $\times$ 52.5 mm. The light exit face has dimensions of 52 mm $\times$ 52.5 mm. The base of this prism is roughly 33.5 mm $\times$ 52.5 mm. The camera lens has a focal length of 50 mm. A tungsten miniature bulb is used as a light source. We found that the chromatic dispersion of the CP has no effect on the image sharpness while performing the experiments with the setup shown in Fig. 8. If someone wants to use mercury green light or laser diodes, the value of the corresponding refractive index n must be substituted in Eq. (3) to design the CP.

Fig. 12. Scanned image of the same thumb print (Fig. 10) on a plane paper.

3. Conclusions

The construction details of the proposed optical system shown in Fig. 8 are discussed in detail. The method suggested for restoring the lengthwise compressed image rays coming from the RP to the normal size and to get the correct finger print image is very simple to implement in a laboratory. The method has the advantages of producing finger prints of true size using any CCD camera whose lens distance from the CCD array can be varied.

The author thanks L. Kameswara Rao, K. R. Gunasekhar, N. Krishna, N. C. Shivaprakash, K. B. Vasantha, K. P. Vasudevan, and G. Babu for their cooperation while conducting these experiments.

References

1. F. Galton, *Fingerprints* (Macmillan, 1892).
2. E. R. Henry, *Classification and Uses of Fingerprints* (Rontledge, 1900).
3. T. Scheimpflug, "Processing of cards and plates using photographic methods," J. Roy. Acad. Sci. Vienna **116,** 235–266 (1907).
4. H. Gross, *Handbook of Optical Systems, Fundamentals of Technical Optics* (Wiley-VCH, 2005), Vol. 1, pp. 475–483 and 632–633.
5. J. M. Sasian, "Image plane tilt in optical systems," Opt. Eng. **31,** 527–532 (1992).
6. S. Igaki, S. Eguchi, F. Yamagishi, H. Ikeda, and T. Inagaki, "Realtime fingerprint sensor using a hologram," Appl. Opt. **31,** 1794–1802 (1992).
7. B. Channankara, W. Y. Xu, F. C. Lin, M. D. Drake, and M. A. Fiddy, "Optical fingerprint recognition using a wave guide hologram," Appl. Opt. **34,** 4079–4082 (1995).
8. M. D. Drake and M. A. Fiddy, "Holographic fingerprint entry device," in October 1995 SPIE International Technical Working Group Newsletter (SPIE, 1995), pp. 6–7.
9. M. D. Drake, M. L. Lidd, and M. A. Fiddy, "Waveguide hologram fingerprint entry device," Opt. Eng. **35,** 2499–2505 (1996).
10. R. D. Bahuguna and T. Corboline, "Prism fingerprint sensor that uses a holographic optical element," Appl. Opt. **35,** 5242–5245 (1996).
11. I. Fujieda and H. Haga, "Fingerprint input based on scattered-light detection," Appl. Opt. **36,** 9152–9156 (1997).
12. J. F. Stephany and W. E. Haas, "Keystone compensation for image storage systems," Appl. Opt. **15,** 1626–1628 (1976).
13. V. M. Duran-Ramirez and D. Malacara-Doblado, "Keystone aberration correction in overhead projectors," Appl. Opt. **43,** 4123–4126 (2004).
14. D. Brewster, *A Treatise on Optics* (Longman, 1831), pp. 363–365.
15. G. H. Cook, "Recent developments in anamorphic systems," J. Soc. Mot. Pict. Tel. Eng. **65,** 151–154 (1956).
16. W. J. Smith, *Modern Optical Engineering: The Design of Optical Systems* (McGraw-Hill, 1966), pp. 239–241.
17. R. Kingslake, *Applied Optics and Optical Engineering* (Academic, 1969), Vol. 5, pp. 7–10.
18. D. Malacara and Z. Malacara, *Handbook of Lens Design* (Marcel Dekker, 1994), pp. 556–557.
19. A. H. Firester, T. E. Gayeski, and M. E. Heller, "Efficient generation of laser beams with an elliptic cross section," Appl. Opt. **11,** 1648–1649 (1972).
20. W. Veldkamp and E. Van Allen, "Compact collinear and variable anamorphic beam compressor design," Appl. Opt. **21,** 7–9 (1982).
21. A. W. Lohmann and W. Stork, "Modified Brewster telescopes," Appl. Opt. **28,** 1318–1319 (1989).